



Optical metrology measurements with HASO™

Imagine Optic, 18 rue Charles de Gaulle, 91400 Orsay, France
contact@imagine-optic.com

APPLICATION NOTE

Imagine Optic offers a wide range of products (hardware and software), which can be used together to accurately characterize the optical quality of a complex optical systems. For instance the wavefront sensors from HASO™ line are perfectly suited for metrological characterization. They can accurately measure distortion, field curvature, wavefront error and optical aberrations. Based on a patented Shack-Hartmann technology, HASO™ wavefront sensors by Imagine Optic contain an association of a microlens grid and a detector in order to calculate local derivatives of the wavefront and this way it can reach the accuracy of $\lambda/100$ RMS (Root Mean Square).

This document presents an example of HASO™ wavefront sensor application to characterize the optical quality of a complex lens.

1. Introduction

This document presents the optical characterization of an imager, which was designed to introduce as little distortion as possible, with a limited amount of aberrations across its field of view. This imager, called complex lens in the following paragraphs, is made of five lenses, as it is shown in **Figure 1**.

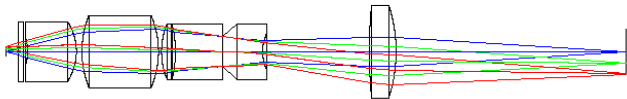


Figure 1. The optical layout of the imager (complex lens).

We chose to use HASO3 128 GE2 in this experiment, because it offers a very high spatial resolution. However, any other HASO™ wavefront sensor from Imagine Optic™ can be used in the same way as we describe here in this note.

2. Experimental set-up

The complex lens, which we characterize in this application note is an objective working at a magnification of 0.2x with a numerical aperture (NA) of 0.3 on the object side. The HASO™ can be used with NA up to 0.1. Thus it may only be used on the image side of the complex lens if no extra optics are added. Then we need an aberrationless light source with a high numerical aperture to place it in the object focal plane of the complex lens. Nevertheless, it cannot be done in our case, because the mechanics of the complex lens hinder the placement of the light source in the object focal plane. The light source then needs to be placed in the image plane of the complex lens. In our case, we simply used a fibered laser diode source. To be able to use the HASO™ on the object side of the complex lens, a microscope objective lens has to be placed between the complex lens and the HASO™. In our case we placed the HASO™ sensor as close as possible to the exit pupil plane of the microscope objective and Imagine Optic's WaveView software was used to extract and process the data from the wavefront sensor.

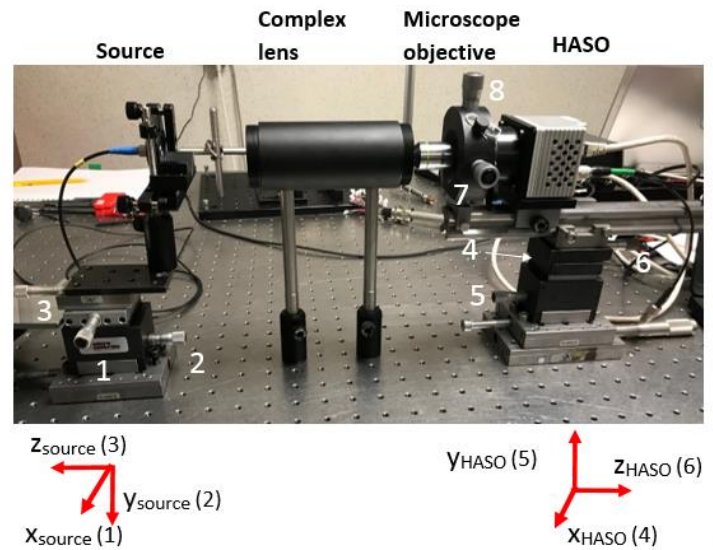


Figure 3. Experimental setup with definition of axes.

Our experimental setup (see **Figure 3**) has total of eight micro-adjusters to align the light source, the microscope objective and the HASO™. The light source is mounted on X_{source} , Y_{source} and Z_{source} translation stages with micro-adjusters **1**, **2** and **3** for alignment. The microscope objective can be moved along x and y, with micro-adjusters **7** and **8** and both the microscope objective and the HASO™ are on a rail, mounted on X_{HASO} , Y_{HASO} and Z_{HASO} translation stages (micro-adjusters **4**, **5** and **6**).

3. Light source alignment without the microscope objective: magnification measurement

In our case, the light source is aligned along the Z_{source} direction when the magnification is 1/5. To find this position, the HASO™ is used **without microscope objective**, as it may be used with converging or diverging beams. Indeed, the position of the focal point of the beam could be determined by the HASO™, and is given by “**X, Y position**” parameters in WaveView, as shown on **Figure 4**.

Note that for a converging (or diverging) beam, the “**Focal point position**” panel of WaveView's Parameters window provides the location of the focal point in the reference frame of the HASO™.

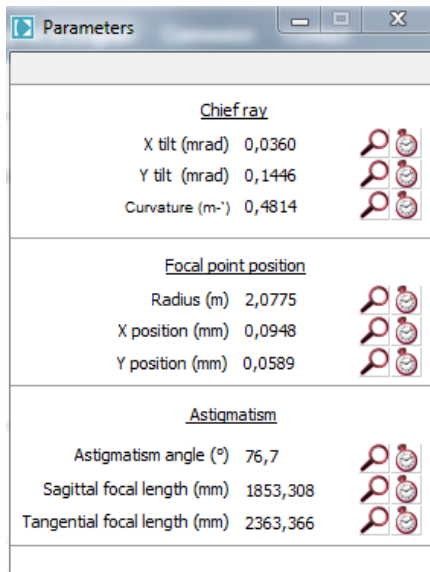


Figure 4. Example of alignment parameters provided by WaveView.

However, for collimated beams, the **“Chief ray”** panel gives useful information concerning the beam’s tilt and curvature. Those parameters, in turn, assist in precise positioning of optical elements by decreasing the tilt values close to zero.

For a fixed position along the z_{source} direction, we move the source by a given distance Δx , obtained by moving micro-adjuster **1** along x_{source} . We then measure the distance $\Delta x'$, given by corresponding **“X position”** values, as shown in **Figure 5** for two measurements along z_{source} . For each z_{source} position, the magnification is then given by $\Delta x'/\Delta x$.

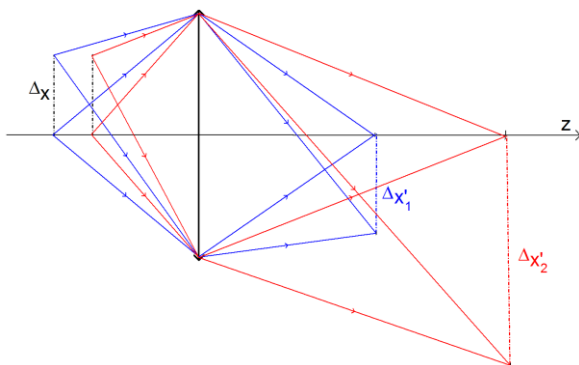


Figure 5. Schematic representation of the magnification measurement, for the conjugation plane localization.

Figure 6. shows magnification measurements for different positions along z_{source} direction, allowing the accurate estimation of the conjugation plane location.

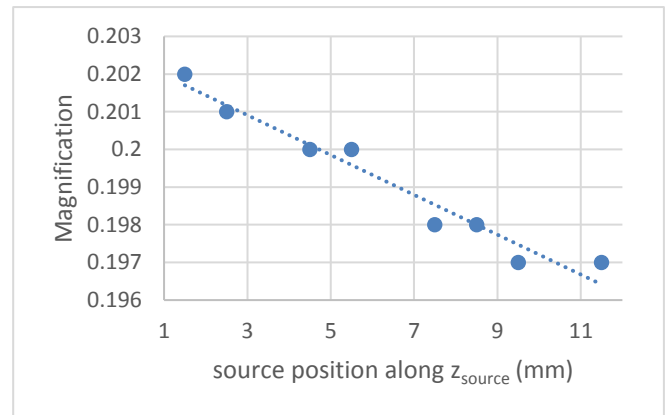


Figure 6. Magnification along z_{source} .

Once the correct conjugation location along z_{source} is determined, it should remain unchanged for the rest of the measurements.

4. Measurements without the microscope objective: field curvature and distortion

Before adding a microscope objective lens to the setup, the field curvature and distortion have to be also measured. To determine the field curvature along x and y , the value of WaveView’s **“Radius”** parameter is plotted for different positions of the source along the x_{source} and y_{source} directions (see **Figure 7**). The minimum radius value is visible around $x_{source} = 15$. This gives a first estimation of the complex lens optical center location along x_{source} .

Distortion results in a magnification change across the field of view. To estimate this change, we first measure the values of **“X position”** for several positions throughout the field along x_{source} , as it is shown in **Figure 8**. Then, to get the local magnification for a point x_{source} , the local magnification is computed, using five measurements: the measurement corresponding to x_{source} , and to the two previous and two following points. The local slope of the linear regression found using these five measurements gives the local magnification at the point x_{source} . **Figure 9** shows the local error in magnification, found by comparing the local magnification and the global magnification. The

local changes in magnification do not show any particular tendency, so we can conclude that distortion is less than 1%.

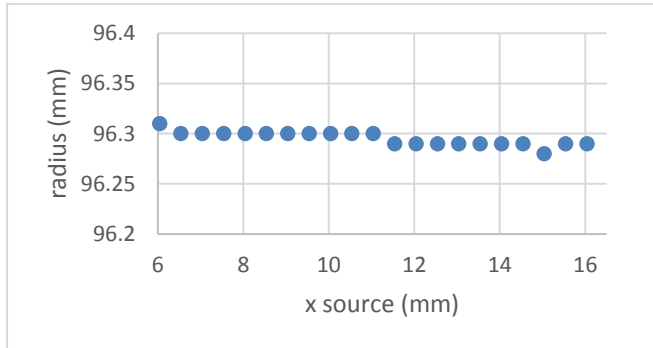


Figure 7. Curvature measurement along x_{source} .

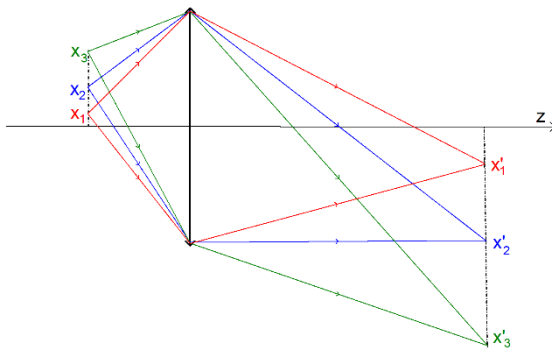


Figure 8. Principle of distortion characterization.

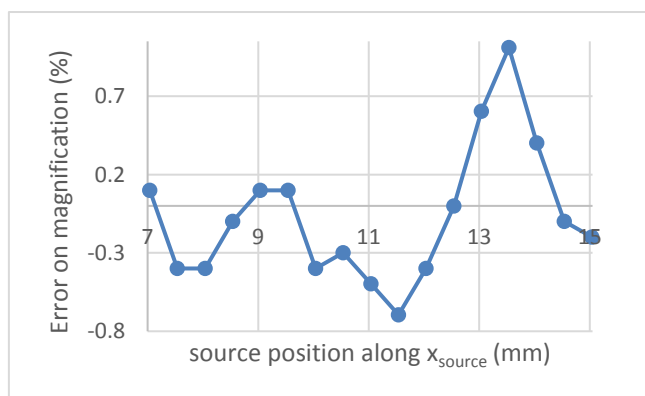


Figure 9. Magnification local error along x_{source} .

5. Alignment of the microscope objective

Once the correct magnification adjustment is achieved, the further optical characterization requires to accurately align the source and the HASO™ through the complex lens. After roughly positioning the light source in the complex lens center, the micro-adjusters **4** and **5** should be used in order to minimize the “(X,Y) positions” parameters inside WaveView software (see **Figure 4**). This procedure ensures that the image plane is centered on the microlens grid. The microscope objective is then added to the optical setup and aligned in respect to the HASO™. The micro-adjusters **7** and **8** are thus used to minimize “(X,Y) tilt” in WaveView software, and should remain unchanged until the end of measurements. Centering the microscope objective ensures that the optical setup is correctly aligned. Nevertheless, it does not prevent from introducing an offset in further metrology measurements. Aberrations induced by the microscope objective should be measured (calibrated) and subtracted before estimation of aberrations induced by the complex lens. This calibration requires a light source with a larger NA than the microscope objective’s one.

6. Optical characterization with the complete setup

The optical set-up is now ready for the localization and characterization of the optical center of the complex lens. This measurement consists in mapping the wavefront error (WFE) across the work field of the complex lens. To do so, the work field is scanned by moving the source (thanks to micro-adjusters **1** and **2**). The HASO™ has to be repositioned (minimizing X and Y tilts with micro-adjusters **4** and **5**) every time the source is displaced. In order to ensure a precise WFE measurement, micro-adjuster **6** shall be used to maintain the radius parameter of WaveView to a constant value. The total wavefront distortion value in RMS (Root Mean Square) is thus directly given by the WaveView software. The location of the optical axis of the complex lens is then set to the coordinates corresponding to the minimum of the WFE value. The WFE map measured for the complex lens is shown in **Figure 10**. This measurement allows us to determine distance between the optical and mechanical axes locations. In our studied complex lens, a discrepancy of 25 % of the field diameter

has been measured between them. As long as its optical center is known, the comparison of the optical model for the complex lens aberrations with WaveView measurements is straightforward. Indeed, WaveView allows us to simply decompose the wavefront using Zernike polynomials, which are known to correspond to classical aberrations. A comparison between aberration's influence across the field has been done. It is displayed as a histogram for different points in the field (see **Figure 11**), or directly as wavefront maps (see **Figure 12** and **13**). At this stage, we can fully characterize the optical quality of the complex lens. Indeed, as it is shown in **Figure 11**, all field aberrations are decreasing when the complex lens is placed closer to the optical axis, except for Coma 90°. This indicates that one or more optical elements inside the complex lens are badly centered.

WaveView offers the opportunity to subtract multiple aberration modes from the wavefront. This allows us to measure the optical quality of the complex lens without centering issues, which are known to introduce mainly the 3rd order aberrations. After subtraction of the 3rd order spherical aberration we observe (see **Figure 13**) that 5th order spherical aberration is now the main aberration induced by this complex lens, but the amplitude of these aberrations is negligible (15 nm RMS on axis and on half-field). However, when observing further in the field of view, by placing the source at a higher field angle, trefoil becomes predominant increasing the total WFE to 20 nm RMS. All these measurements can thus be compared with the optical model of the complex lens in order to validate its fabrication.

7. Conclusion

We used HASO3 128 GE2 produced by Imagine Optic to qualify the optical quality of a customized imager. The high precision of HASO3 128 GE2 allowed us to accurately measure the distortion, curvature and wavefront aberrations induced by the complex lens. These measurements have been used to find the optical axis of complex lens with a great precision and allowed us to locate the excentricity defect inside this optical system, which is caused by the faulty mechanical structure inside the complex lens.

For more information, and to find the Imagine Optic's office or distributor nearest to you, please visit www.imagine-optic.com

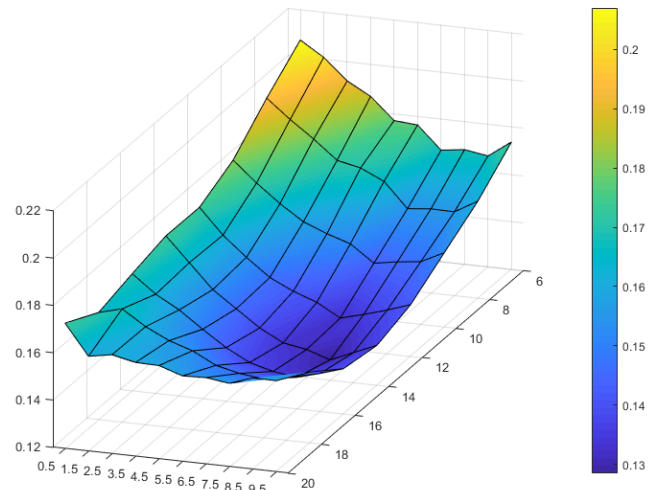


Figure 10. Complex lens WFE measurement in the work field. Axes (xOy) stands for the field coordinates, in mm, and the axis (Oz/colormap) stands for the global RMS (Root Mean Square) WFE, in μm .

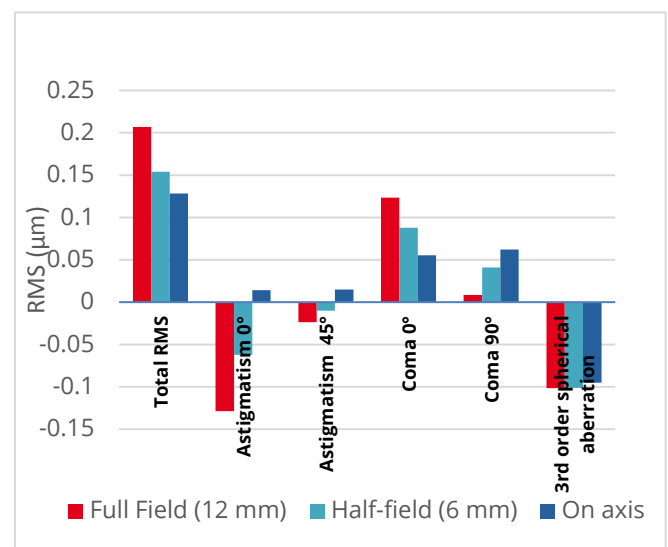


Figure 11. Wavefront decomposition over the 3rd order aberrations. The presence of Coma in the center of the field points out a centering issue due to one or more optics in the complex lens. Higher order aberrations are negligible compared to 3rd order aberrations.

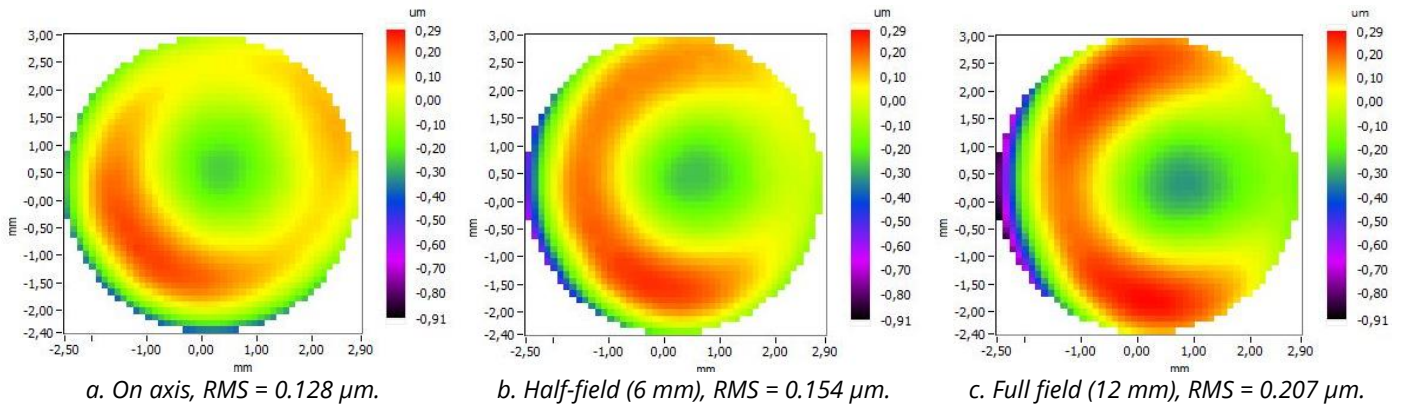


Figure 12. Wavefront evolution accross the work field. Coma is significant on axis, which is characteristic of an excentricity defect. Astigmatism appears with the field and prevails at the edge of the field.

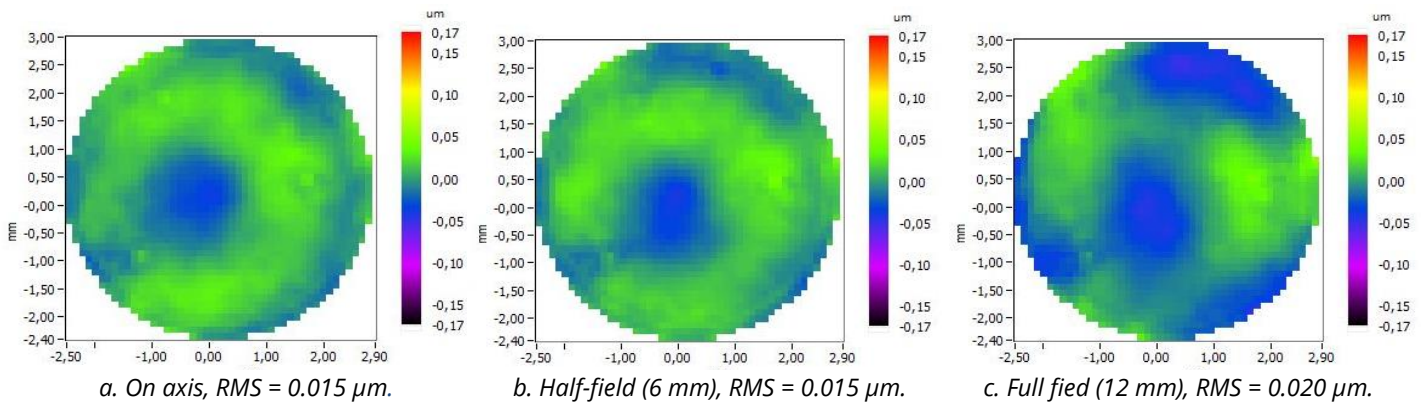


Figure 13. Wavefront evolution accross the work field, without the 3rd order aberrations influence. The 5th order spherical aberration is predominant on axis, but the trefoil prevails at the edge of the work field.